Cu(II) organizes β-2-microglobulin oligomers but is released upon amyloid formation

KWASI ANTWI, MAURA MAHAR, RAPOLE SRIKANTH, MARK R. OLBRIS, JULIAN F. TYSON, AND RICHARD W. VACHET

Department of Chemistry, University of Massachusetts Amherst, Amherst, Massachusetts 01003, USA

(RECEIVED September 18, 2007; FINAL REVISION January 2, 2008; ACCEPTED January 2, 2008)

Abstract

β-2-Microglobulin (β2m) is deposited as amyloid fibrils in the bones and joints of patients undergoing long-term dialysis treatment as a result of kidney failure. Previous work has shown that biologically relevant amounts of Cu(II) can cause β2m to be converted to amyloid fibrils under physiological conditions in vitro. In this work, dynamic light scattering, mass spectrometry, and size-exclusion chromatography are used to characterize the role that Cu plays in the formation of oligomeric intermediates that precede fibril formation. Cu(II) is found to be necessary for the stability of the dimer and an initial form of the tetramer. The initially formed tetramer then undergoes a structural change to a state that no longer binds Cu(II) before progressing to a hexameric state. Based on these results, we propose that the lag phase associated with β2m fibril formation is partially accounted for by the structural transition of the tetramer that results in Cu(II) loss. Consistent with this observation is the determination that the mature β2m amyloid fibrils do not contain Cu. Thus, Cu(II) appears to play a catalytic role by enabling the organization of the necessary oligomeric intermediates that precede β2m amyloid formation.

Keywords: β-2-microglobulin; copper; amyloid; dialysis-related amyloidosis; mass spectrometry; dynamic light scattering; size-exclusion chromatography

While protein amyloid fibril formation is associated with human diseases such as Alzheimer's, Parkinson's, light-chain amyloidosis, type II diabetes, and many others (Rochet and Lansbury Jr. 2000), the mechanisms by which soluble proteins progress into insoluble amyloid fibrils are still not clear. Understanding the mechanisms of these processes has great importance not only for explaining these biological phenomena but also for rationally addressing these diseases.

β-2-Microglobulin (β2m) is a small protein (~12 kDa) subunit of the class I major histocompatibility (MHC) complex (Bjorkman et al. 1987). Upon turnover of the MHC complex, the major fraction of β2m is normally degraded in the kidney. While the plasma concentrations in people with healthy kidneys are typically 1–3 mg/L, elevated levels (10–60 times) of β2m can be found in people suffering from kidney disease (Drüeke 2000; Floege and Ketteler 2001). β2m is thought to be present physiologically as a monomer; however, its amyloid formation and subsequent deposition in joints and connective tissues are complications of severe renal failure

Reprint requests to: Richard W. Vachet, Department of Chemistry, University of Massachusetts Amherst, Lederle GRT 701, 710 North Pleasant Street, Amherst, MA 01003, USA; e-mail: rwvachet@chem.umass.edu; fax: (413) 545-4490.

Abbreviations: β2m, β-2-microgobulin; MHC, major histocompatibility complex; DRA, dialysis-related amyloidosis; MOPS, 3-(N-morpholino)propanesulfonic acid; EDTA, ethylenediamine tetraacetic acid; SEC, size-exclusion chromatography; MW, molecular weight; MS, mass spectrometry; ESI, electrospray ionization; DLS, dynamic light scattering; ThT, thioflavin T; TEM, transmission electron microscopy; ICP, inductively coupled plasma; FESEM, field emission scanning electron microscope; SDS, sodium dodecyl sulfate; ppm, part per million.

Article published online ahead of print. Article and publication date are at http://www.proteinscience.org/cgi/doi/10.1110/ps.073249008.

and long-term dialysis treatment, leading to a condition referred to as dialysis-related amyloidosis (DRA). Elevated concentrations alone, though, are not sufficient for conversion of β2m to amyloid fibrils. Other factors, caused presumably by the dialysis procedure, are necessary.

While the exact factors that cause β2m fibril formation in vivo are not known, several means exist to generate β2m amyloid fibrils in vitro. β2m amyloid fibrils can be generated under acidic conditions (pH < 3.6) (McParland et al. 2000), by truncating the first six N-terminal amino acids (Esposito et al. 2000), by dialyzing the protein into distilled water followed by membrane drying (Connors et al. 1985), by mixing the protein with collagen at pH = 6.4 (Relini et al. 2006), by sonicating the protein in the presence of sodium dodecyl sulfate at pH = 7.0 (Ohhashi et al. 2005), and by incubating the full-length protein at physiological conditions in the presence of stoichiometric amounts of Cu(II) (Morgan et al. 2001; Eakin et al. 2002). The latter method is intriguing and may have relevance to the in vivo process because of the very near physiological conditions used. Miranker and coworkers have argued that the amount of Cu(II) in the dialysate may be sufficient for Cu(II) to play a causative role in β2m fibril formation in vivo (Morgan et al. 2001; Eakin and Miranker 2005). In a wider context, transition metals, particularly Cu(II), have been found to associate with proteins of several amyloid systems, including Aβ of Alzheimer's disease (Bush and Tanzi 2002), α-synuclein of Parkinson's disease (Uversky et al. 2001), the prion protein of Creutzfeldt-Jakob's disease (Wadsworth et al. 1999; Jobling et al. 2001), and the immunoglobulin light chains in light-chain amyloidosis (Davis et al. 2001). These observations suggest that Cu(II) could play an important general role in the amyloid formation of other systems as well.

Because of the general role that Cu(II) could play in amyloid formation and the specific role that it does play in β2m amyloid formation in vitro, a greater understanding of the molecular features of copper's association with β2m prior to amyloid formation is important to obtain. Previous results indicate that Cu(II)-induced β2m amyloid formation involves structural as well as oligomeric changes prior to fibril formation (Eakin et al. 2004, 2006). Cu(II) was also very recently shown to cause the oligomerization of β2m to a kinetically stable oligomeric form that does not contain Cu(II) (Calabrese and Miranker 2007), suggesting that Cu(II) could play a catalytic role in β2m fibril formation. In our work, we have determined the temporal and stoichiometric progression of β2m oligomers. The role of Cu(II) in the oligomeric changes that precede fibril formation is also determined by resolving the Cu(II)-binding stoichiometries of specific oligomeric intermediates.

Results

Oligomerization of β2m

β2m fibril formation was stimulated using stoichiometric amounts of Cu(II) under conditions almost identical to those reported by Miranker and coworkers (Morgan et al. 2001; Eakin et al. 2002). Thioflavin T (ThT) binding, sodium dodecyl sulfate (SDS) dissolution, and transmission electron microscopy (TEM) imaging were used to confirm that amyloid formation occurred under the incubation conditions in the presence of Cu(II). Upon binding to amyloid-like species, the characteristic fluorescence spectrum of ThT changes (Naiki et al. 1989). Figure 1 shows the ThT fluorescence enhancement upon incubation of monomeric β2m with and without Cu(II). The fluorescence signal produced by the Cu(II)-containing solution begins to increase very soon after Cu(II) is added and levels off after about 1 h. No further increase in the ThT fluorescence is observed even up to 4 d, when the first insoluble material is observed, or after 1 wk when the first indication of amyloid fibrils is seen by TEM. Interestingly, as will be evident from the data below, the shift in ThT fluorescence occurs as soon as a β2m dimer is present in solution, which raises the question of ThT's utility as an indicator of the formation of β2m amyloid-like species. In contrast, no ThT fluorescence enhancement is observed in the control reaction [i.e., no Cu(II) present] for any time point up to 1 wk. Moreover, no observable insoluble material is formed in the absence of Cu(II) for up to 2 mo. These results are consistent with those observed previously and indicate that Cu is necessary to stimulate the formation of amyloid-like species.

Another characteristic feature of amyloid-like aggregates as opposed to amorphous aggregates is that they do not readily dissolve in 2% SDS. To test whether the insoluble aggregates that are formed after 1-wk, 2-wk,

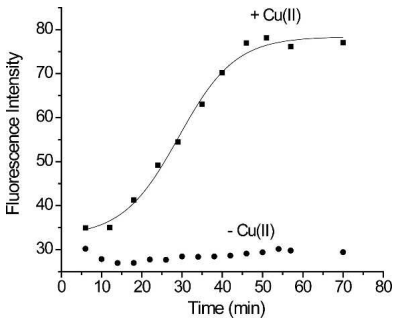

Figure 1. β2m amyloid formation monitored by thioflavin T (ThT) fluorescence at 483 nm. The ThT fluorescence maximum shifts from 450 nm to 483 nm upon binding to amyloid-like structures, and the fluorescence intensity at 483 nm increases in the presence of Cu (■) but remains the same in the absence of Cu (●). The trend line associated with the Cu data is from a sigmoidal fit of the data.

and 1-mo incubations with Cu(II) have this characteristic, the aggregates were filtered and added to a 2% solution of SDS at 37°C. In all the samples incubated for at least 1 wk, a visual assessment of the insoluble material indicated that the aggregates did not dissolve after 24 h in the presence of SDS, indicating that they were amyloid-like aggregates. Finally, TEM images of the aggregates were taken after incubation with Cu(II) for different time periods (Fig. 2). After 1 wk (Fig. 2A) of incubation, most aggregates do not have well-defined structures, but a few do have straight morphologies. After 2 wk (Fig. 2B), most aggregates have curved and worm-like structures, and more straight fibrils are observed. After 3 wk (Fig. 2C), most of the fibrils have long and straight morphologies, which are hallmarks of amyloid fibrils; however, some curved or worm-like structures are also still observed. After 1 mo of incubation (Fig. 2D), the vast majority of the fibrils are long and straight. Taken as a whole, the ThT fluorescence measurements, SDS dissolution experiments, and TEM images suggest that the aggregates formed during incubation with Cu(II) are amyloid in nature. Thus, with proper incubation conditions that result in amyloid formation, further experiments were carried out to characterize the oligomeric intermediates formed prior to fibril formation.

Characterization of oligomeric intermediates

Dynamic light scattering (DLS), mass spectrometry (MS), and size-exclusion chromatography (SEC) were used to characterize the oligomeric intermediates that form prior to fibril formation. These techniques are complementary tools as they provide related information about oligomeric forms. Importantly, when data from these three techniques are consistent, then confidence in the data from each is increased. Results from each of these tools led to two general observations about the oligomeric intermediates: (1) β2m forms dimers, tetramers, and hexamers; (2) dimers, tetramers, and hexamers are measured in solution before amyloid fibrils are observed.

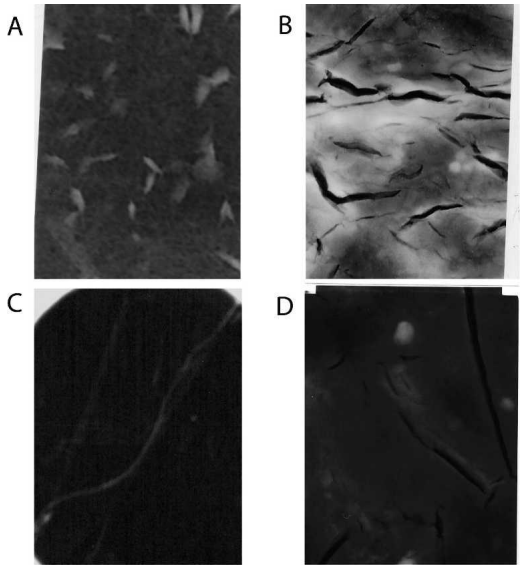

Figure 2. Transmission electron micrograph images obtained from β2m samples after incubation with Cu(II) for (*A*) 1 wk, (*B*) 2 wk, (*C*) 3 wk, and (*D*) 4 wk. Dimensions of images *A–C* are 200 nm × 325 nm, and dimensions of image *D* are 500 nm × 800 nm.

DLS data (Fig. 3) during the first 15 d of the incubation with Cu(II) indicates that dimers, tetramers, hexamers, and occasionally dodecamers are formed. A DLS measurement of a buffered solution of un-incubated monomeric β2m gives a radius of 2.0 nm, which compares favorably with the estimated size of β2m in solution (Verdone et al. 2002). As β2m is incubated in the presence of Cu(II), compounds with scattering distributions centered at 2.3, 4.8, 8.7, 12.7, and 28.2 nm are observed over time; however, the compound with a scattering radius of 28.2 is not always observed. Also, a compound with a radius of 55 nm, which would roughly have 24 β2m units, is occasionally observed, but it is excluded from Figure 3 because it is rarely seen. Particles with radii greater than 100 nm are also occasionally observed, but these particles were usually ignored in the analyses as they were most prevalent (and sometimes completely dominated the signal) when samples were agitated too much before the DLS measurement. A scattering radius of 2.3 nm is similar to 2.0 nm, which suggests that this compound is monomeric β2m. Given this radius for the monomer, the compounds with radii of 4.8, 8.7, 12.7, and 28.2 nm are likely dimers, tetramers, hexamers, and dodecamers, respectively. Interestingly, no compounds with radii corresponding to trimers, pentamers, heptamers, etc., are readily apparent. In summary, the DLS data indicate that monomeric β2m first forms a dimer, and then higher-order oligomers are formed via the assembly of dimeric units.

Mass spectral data of Cu(II)-incubated samples up to day 7 confirm that dimers, tetramers, and hexamers are formed, while no odd numbered higher-order oligomers are seen. Mass spectra of control samples up to 7 d only show monomers (data not shown). Figure 4A is a representative electrospray ionization (ESI) mass spectrum from a sample that was incubated for 5 d in the presence of Cu(II). The resolution in this spectrum is poor because low-energy ESI source conditions were chosen to minimize oligomer dissociation. Under these ion source conditions many adducts from the desalted incubated solution remain, and these adducts, which are mostly due to ammonium acetate clusters, broaden the mass spectral peaks for all the oligomers. Despite this peak broadening, different oligomeric species can be identified

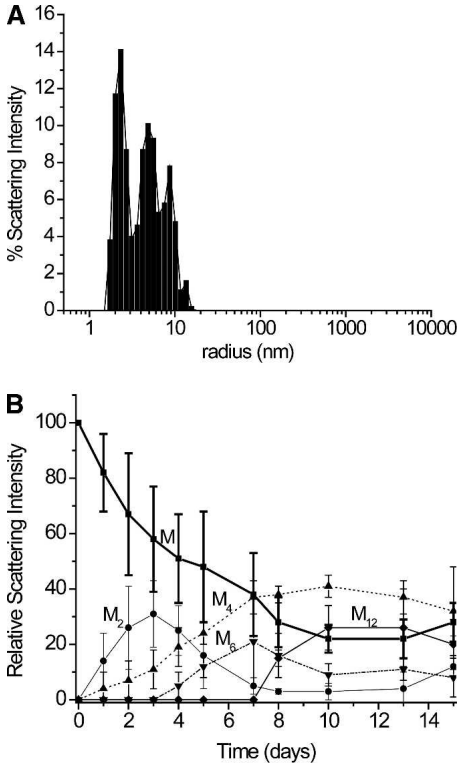

Figure 3. DLS analysis of β2m oligomer sizes after incubation with Cu(II). (*A*) Scattering intensities as a function of radii for a Cu-β2m sample incubated for 4 d. (*B*) Temporal progression of β2m oligomers for the first 15 d of an incubation in the presence of Cu(II). Monomers (M), dimers (M_2), tetramers (M_4), hexamers (M_6), and dodecamers (M_{12}) are observed. The error bars represent the standard deviations from three replicate measurements, except for the dodecamers, which were not observed in all measurements. At days 13 and 15, particles with scattering radii of >100 nm were consistently measured, but these species are not included in this plot. The lines connecting the data points are not fits of the data but are provided to simplify visualization of the data.

given that the molecular weight of monomeric β2m is 11,731. Peaks that appear at *m*/*z* ratios around 2135, 2350, and 2610 (labeled "M_2") are the +11, +10, and +9 charge states of the dimer and confirm its presence. The +11 and +9 charge states particularly identify these series of peaks as dimers because monomers with these *m*/*z* ratios would have the impossible charge states 5.5 and 4.5. Similarly, peaks at *m*/*z* ratios around 2760 (+17), 2940 (+16), 3130 (+15), and 3360 (+14) (labeled "M_4") indicate the presence of a tetramer. The presence of hexamers is suggested by weakly abundant ions at *m*/*z* ratios around 3705 (+19), 3915 (+18), and 4150 (+17) (labeled "M_6"), but these data are not conclusive. Like the DLS data, no consistent evidence for odd-ordered oligomers is found in the mass spectral data for samples incubated up to 7 d.

To improve the resolution of the spectrum and improve our confidence in assigning the spectral peaks, especially for the hexamers, other spectra were obtained under higher-energy ESI conditions (e.g., Fig. 4B). This spectrum more clearly indicates the presence of dimers, tetramers, and hexamers. Also, now present are peaks that are consistent with a trimer and possibly a pentamer.

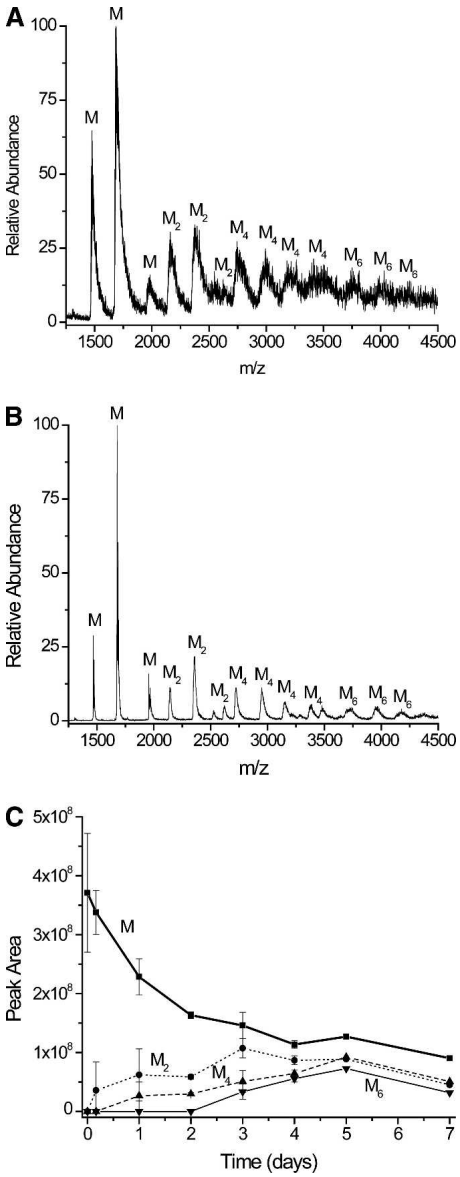

Figure 4. Mass spectral data for β2m incubated with Cu(II) after desalting. (*A*) Mass spectrum obtained after a 5-d incubation, taken under low-energy ESI source conditions. (*B*) Mass spectrum obtained after a 5-d incubation, taken under high-energy ESI source conditions. (*C*) Ion abundances of β2m oligomers obtained over time. The ion abundance of each oligomer is the sum of the peak areas for each charge state of that oligomer. To account for day-to-day variability in the ion signal from the ESI source, the mass spectrum of a 5 μM solution of ubiquitin was analyzed immediately before the incubated sample. β2m oligomer ion abundances were then normalized to the ubiquitin ion signals each day so that the oligomer ion abundances could be compared from one day to the next.

Because these peaks are not apparent in other mass spectra (days 1–7) taken under the low-energy ESI conditions, we conclude that these peaks are artifacts that arise from dissociation of some of the tetramers or hexamers in the ESI source. Indeed, the trimer peaks are not detected even under higher-energy ESI conditions until day 3, and the potential pentamer peak is only observed at day 5. Thus, like the DLS data, the MS results indicate that β2m oligomers are formed through the building up of dimeric units. Figure 4C shows the formation of the different oligomers over time as measured by MS. The data from this plot are roughly consistent with the DLS data shown in Figure 3. In particular, both sets of data show that dimers are formed as soon as the measurements can be made, tetramers are first formed after 24 h, and the hexamer is formed after day 3. Considered together, the DLS and MS data indicate that dimers, tetramers, and hexamers are all formed in solution prior to observing insoluble material or β2m fibrils.

SEC analyses indicate the presence of monomers, dimers, tetramers, and higher molecular-weight oligomers when incubated Cu-β2m samples are analyzed over the course of 2 wk (Fig. 5A,B). Based on comparison to a calibration curve, the molecular weights of the compounds that have elution times of 38, 35, and 29 min (Fig. 5A) are estimated to be 11,730, 18,400, and 45,200, respectively. The compound(s) that have an elution time of 19 min have molecular weights greater than or equal to 100,000. No more precise information is available for these latter compounds because they are at the exclusion limit for the column. The expected molecular weight of the monomer is 11,731, which matches the molecular weight of the peak at 38 min, so this peak was assigned to the monomeric protein. This assignment was also confirmed by online SEC-MS analysis (data not shown). The estimated molecular weight of the peak at 35 min (18,400) is much less than the expected molecular weight of the dimer (23,458); however, online SEC-ESI-MS analysis confirmed that it was the dimer (Fig. 5C). The peak at 29 min has an estimated molecular weight of 45,200, which is about 10,000 more than the expected molecular weight of the trimer and about 1700 less than the expected molecular weight of the tetramer, which gives us good confidence that this peak corresponds to the tetramer. Online SEC-ESI-MS analysis confirms this assignment (data not shown) and indicates that a small amount of hexamer co-elutes with the tetramer as ions for this hexamer are measured. This observation indicates that our SEC column is not efficient enough to resolve the tetramer from the hexamer, suggesting that the hydrodynamic radii of the tetramer and hexamer are similar. When compared to the DLS and MS data, the intensities of the oligomers from the SEC analyses are relatively low. In contrast to the DLS and MS data, the

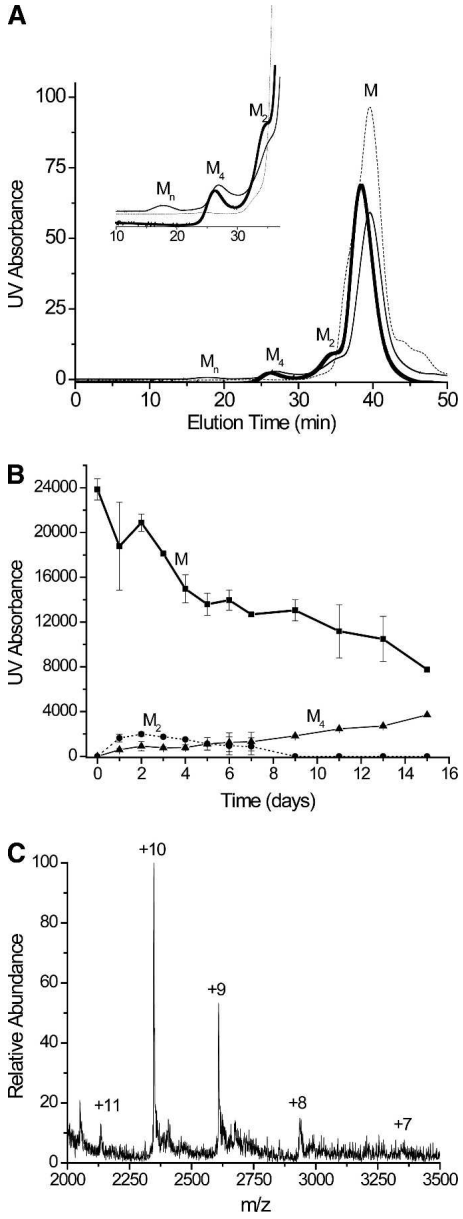

Figure 5. SEC analysis of incubated β2m sample. (*A*) Example chromatograms for a control [i.e., no Cu(II)] sample (dotted line), a sample incubated for 2 d with Cu(II) (thick line), and a sample incubated for 4 d with Cu(II) (thin line). The *inset* shows an expanded region of the chromatogram from 10 to 37 min. Monomers (M), dimers (M_2), tetramers (M_4), and oligomers with molecular weights above 100,000 (M_n) are observed. (*B*) Temporal progression of the oligomers measured by SEC. The high molecular weight oligomers (M_n) are not included in this plot. (*C*) SEC-ESI mass spectrum of the chromatographic peak eluting at 35 min, confirming that this compound is the β2m dimer. The charge state of each mass spectral peak is labeled.

SEC measurements take place >25 min after the oligomers have been removed from the incubated solution. Because the oligomers are physically separated in SEC and are no longer in equilibrium, they can dissociate before being

detected >19 min after injection. The reduced intensities are then likely due to oligomer dissociation; however, the data in Figure 5A do indicate that some fractions of the oligomers are stable for >25 min.

Evolution of oligomers

Close examination of the DLS data (Fig. 3) reveals some interesting aspects about the dynamics of the oligomer formation. These data cannot be used to quantitatively assess the relative amounts of each oligomer because larger compounds scatter more light than smaller compounds. Even so, the temporal changes in the amount of scattered light by each individual oligomer are insightful. The oligomerization process occurs by first forming a dimer, whose concentration becomes greatest around day 3. Tetramer is not observed until day 1, and its abundance appears to increase as more dimer is formed. This observation and simple reason indicate that the dimer is a necessary precursor to the formation of the tetramer. In contrast, the tetramer is present for 2 or 3 d before the hexamer is observed. The MS data show a similar result (Fig. 4C). This observation implies that the tetramer is initially incapable of progressing to the hexamer, but something happens to the tetramer (e.g., a conformational change) around day 3 that allows it to progress to a hexamer. Once the hexamer is formed in solution, the concentration of the dimer decreases to almost zero, which suggests that the hexamer formation requires the dimer. Accompanying the appearance of the hexamer and the initial decrease in dimer concentration is the first evidence of insoluble material. Furthermore, the first evidence of amyloid-like fibrils by TEM occurs at 1 wk, which coincides with the maximum hexamer concentration. These results might suggest that an oligomer just larger than the hexamer is the unstable nucleus that promotes fibril or protofibril formation. Additional evidence that supports this idea is the fact that octamers and decamers are not observed in solution. The point at which the concentration of hexamer is greatest in solution (day 7) is also the point at which the concentration of monomer sharply decreases and the concentration of tetramer begins to level off. The leveling off of the tetramer concentration may be explained by the need for the tetramer to undergo a conformational change to form a hexamer, as speculated above. This speculation suggests that the tetramer has two forms, one that is capable of progressing to a hexamer and one that is not.

Role of Cu(II) in the stability of oligomeric intermediates

Cu(II) is clearly important for fibril formation, but its specific role in the formation and stability of the oligomeric intermediates is important to assess. SEC and MS were used to gather insight into Cu(II)'s association with each oligomer. Cu appears to be necessary for the stability of the dimer and the tetramer up to about day 5. This observation is apparent after 10 mM EDTA is added to an aliquot of the incubation solution just before SEC analysis. With the addition of EDTA, only the monomer is observed by SEC up to day 5 (Fig. 6). This result indicates that once Cu(II) is extracted from the dimer and the tetramer, they are no longer stable (up to day 5) and subsequently revert back to the monomer. However, at day 5, some fraction of the tetramer peak remains after reaction with EDTA. Even after allowing EDTA to react with the sample for 60 min, this fraction remains. Because the tetramer and hexamer co-elute in SEC, MS of the EDTA-treated solutions was also performed; however, while the tetramer is observed by MS, the low MS signal for the EDTA-treated samples does not allow us to confidently conclude whether or not the hexamer is still present (data not shown). Other recent work on β2m reported a similar transition after about 5 d (Calabrese and Miranker 2007); our work allows these oligomers to be identified as tetramers, but we cannot rule out the additional presence of hexamers. Thus, it appears that there are two tetrameric forms: one requiring Cu(II) and one that does not require Cu(II). This observation is consistent with the data described in the previous section, which suggested the presence of two forms of the tetramer: one that progresses to hexamer after day 4 and one that continues to increase in concentration up to day 10 (Fig. 3). Finally, while removal of Cu causes the dimer and tetramer to revert back to monomer, once fibrils are formed, incubation with EDTA does not reverse the fibrils back to monomers.

MS data confirm that the monomer, dimer, and tetramer bind Cu(II). Expanded regions of the mass spectra around the +7 charge state of the monomer, the

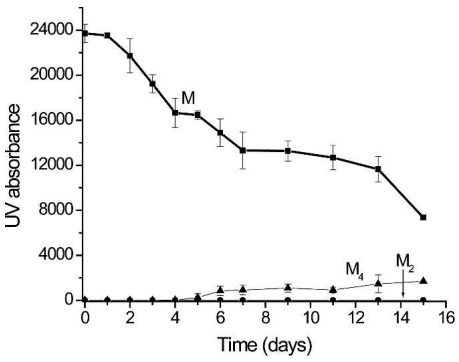

Figure 6. SEC analysis of incubated β2m sample after the addition of EDTA. Samples were incubated for the indicated time, and just prior to analysis, an aliquot of the sample was reacted with 10 mM EDTA. The plot shows data for the monomer (M), dimer (M_2), and tetramer (M_4).

+11 charge state of the dimer, and the +15 charge state of the tetramer (Fig. 7A–C) show that these oligomers bind up to 1, 2, and 4 Cu ions, respectively. These spectra are expanded regions of the spectra acquired under higher-energy ESI source conditions (i.e., Fig. 4B). While the peaks in Figure 7, B and C, are not fully resolved, the high mass accuracy of the double-focusing mass spectrometer that was used increases our confidence in these assignments. For example, the expected *m/z* ratio of the +7 charge state of monomeric β2m is 1676.86, and that of its Cu(II)-bound form is 1685.64. The experimentally measured *m/z* values for these ions are 1676.80 and 1685.57, respectively. Not only are these values very close to the predicted values, they also confirm that Cu(II) and not Cu(I) is bound to the protein. Upon binding to the protein, Cu(II) is expected to replace two protons in order to maintain the same +7 charge state. Cu(II) binding then should increase the mass of the protein by 61.53 mass units (i.e., 63.55 − 2.02; because the resolution in Fig. 7 is not high enough, the average mass of Cu and H are used here). A mass increase of 61.53 will result in an *m/z* increase of 8.79 (or 61.53/7). The observed *m/z* increase of 8.77 is thus very consistent with the Cu(II) binding. Binding by Cu(I) would lead to a *m/z* increase of 8.93. A similar evaluation can be done for the dimer and tetramer shown in Figure 7, B and C, and the measured *m/z* ratios for the relevant peaks are shown in Fig. 7. In both cases, the relatively high mass accuracies observed in these measurements confirm that a maximum of two Cu(II) ions bind to the dimer and a maximum of four Cu(II) ions bind to the tetramer. Unfortunately, the low signal-to-noise ratios of the hexameric peaks and the significant adduct formation associated with these oligomers make it difficult to identify whether the hexamer binds Cu(II). MS analyses of the EDTA-treated samples indicate that the tetramer that remains after day 5 does not contain Cu(II). To confirm that Cu(II) binding to the β2m oligomers is specific and not simply due to ESI-promoted adduct formation, ESI mass spectra of lysozyme, which is a non-Cu-binding protein, were investigated. Upon performing ESI-MS under identical conditions from a desalted sample of lysozyme, no Cu-lysozyme adducts are observed (data not shown). Indeed, no Cu-lysozyme adducts are observed even up to 4:1 Cu:lysozyme ratios.

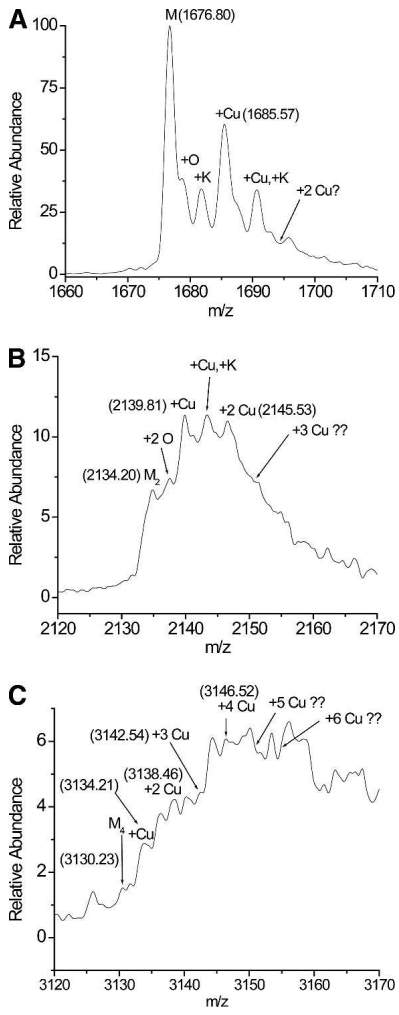

Figure 7. Expanded regions of the mass spectrum for a desalted solution of incubated β2m obtained under high-energy ESI conditions. (*A*) Expanded region around the monomer, indicating the binding of 0 and 1 Cu(II) ion. (*B*) Expanded region around the dimer, indicating the binding of 0, 1, and 2 Cu(II) ions. (*C*) Expanded region around the tetramer, indicating the binding of 0, 1, 2, 3, and 4 Cu(II) ions. In each spectrum the numbers in parentheses are the *m/z* ratios of the corresponding ion.

Further study of Cu binding to β2m was performed by determining if the mature fibrils incorporate Cu. Two sets of data indicate that Cu is not incorporated into the mature fibrils. First, ICP-MS was used to determine the concentration of Cu left in solution after 40 d of incubating β2m under fibril-forming conditions. After this time period, >99% of the soluble protein had been converted into insoluble fibrils. The concentration of Cu found in the remaining solution was 10.2 ± 0.3 parts per million (ppm), which is close to the expected 12.7 ppm that would be found if no Cu was incorporated into the fibrils. The remaining 2.5 ppm of Cu could be incorporated into the fibrils, but control experiments indicate that the remaining Cu has precipitated as $Cu(OH)_2$. Incubating a β2m-free control sample for 40 d, in which all other solution components were present, resulted in a solution Cu concentration of 1.26 ± 0.02 as measured by ICP-MS. Clearly this concentration was much lower than the expected 12.7 ppm and indicates that Cu had precipitated, probably as $Cu(OH)_2$. Indeed, a rinse of the control sample tube with 5 M nitric acid resolubilized >95% of the Cu. Equilibrium calculations confirm that the majority of Cu(II) is expected to precipitate as $Cu(OH)_2$ in the

absence of the protein. Thus, we conclude that the 2.5 ppm of Cu that was not accounted for in the β2m incubated sample precipitates as $Cu(OH)_2$ during the course of the 40-d incubation. A much lower amount precipitated (2.5 ppm) than was observed in the β2m-free control sample, but this was most likely due to the fact that soluble β2m, which was present for much of the incubation period, slowed precipitation of Cu.

A second experiment using X-ray microanalysis was also performed on the fibrils themselves to determine if Cu is incorporated into this insoluble material. Analysis of a ~1 mg sample of the fibrils, after several rinses with buffer, resulted in no measurable Cu. If all the solution Cu had been incorporated into the solid fibrils, then 12.7 μg would have been present. Even though the detection limit for Cu has not been determined for the instrument that was used, this concentration (i.e., 12,700 ppm) should be readily measurable by X-ray microanalysis. X-ray microanalysis of biological samples typically provides detection limits between 100 and 500 ppm for most elements and even lower limits for transition metals (Goldstein et al. 1992). If the amount of Cu unaccounted for in the ICP-MS experiments had been incorporated into the fibrils, then 2.5 μg (or 2500 ppm) would have been present. Again, this concentration should be easily detectable by X-ray microanalysis, so the failure to observe Cu indicates that it is not present in the fibrils.

Discussion

Characterizing reaction intermediates is essential for more deeply understanding any chemical or biochemical reaction, and this is no less true for amyloid fibril-forming reactions. The DLS, MS, and SEC experiments reported here indicate that the formation of β2m fibrils is preceded by the formation of oligomeric intermediates that include dimers, tetramers, and hexamers. No odd-ordered oligomers appear to be precursors, and this observation indicates that the oligomeric intermediates form via the assembly of dimers. These observations are consistent with previous results in which analytical ultracentrifugation was used to identify oligomers formed prior to Cu-induced β2m fibril formation (Eakin et al. 2004). The results presented here provide higher resolution data confirming the presence of these even-ordered oligomers, but our results also elucidate the Cu content of these oligomers and indicate the temporal progression of these oligomers. The formation of discrete oligomers as prefibrillar intermediates has been observed for several other amyloidogenic proteins, too (Walsh et al. 1997; Friedhoff et al. 1998; Ferrao-Gonzales et al. 2005), and indeed acid-induced (pH = 2.5) amyloid formation of β2m has been found to be preceded by dimers, trimers, and tetramers (Smith et al. 2006). The fact that several amyloidogenic proteins form oligomeric intermediates prior to fibril formation may be important because the oligomers themselves might be therapeutic targets for preventing amyloid fibril formation. Indeed, at least in the case of the amyloid β-protein of Alzheimer's disease, oligomeric forms may represent the toxic form (Kirkitadze et al. 2002).

In addition to confirming the presence of even-ordered oligomeric intermediates prior to β2m fibril formation, several experimental observations provide new insight into Cu's role in the formation of the prefibril oligomers. First, MS data confirm that the +2 oxidation state of Cu is the relevant state when complexed to the dimers and tetramers. This may not be surprising as Cu(II) is added to stimulate β2m fibril formation, but the absence of any evidence for Cu(I) suggests that redox processes are unlikely to play a role in the oligomerization and eventual fibril formation of β2m. Oxidation can cause proteins to aggregate, and any reduction of Cu(II) to Cu(I) would likely result in protein oxidation. Not only do we not detect Cu(II) reduction, but mass spectral data show no increase in protein oxidation to the monomer or any of the oligomers over the course of 7 d. As seen most clearly in Figure 7A, the addition of a single oxygen atom to the protein is observed, but the fraction of protein that is oxidized remains at about 20%–30% from day 0 to day 7. Furthermore, tryptic digestion of soluble β2m and peptide sequencing by tandem MS indicate that only Met99 is oxidized after incubations with Cu(II) for periods up to 7 d (J.D. Bridgewater and R.W. Vachet, unpubl.).

Second, Cu(II) binding is necessary for the stability of the dimer and the initial form of the tetramer. Unfortunately, Cu(II)'s role in stabilizing the hexamer is unclear. The importance of Cu for the stability of the dimer and tetramer was obtained by sequestering Cu(II) at different time points during the incubation and by measuring Cu(II) complexes of these oligomers. Sequestering Cu(II) in the β2m incubated sample was achieved by adding an excess of EDTA. EDTA has a much higher affinity for Cu(II) than that estimated for monomeric β2m (Morgan et al. 2001), and given its relatively high concentration (10 mM vs. 100 μM) it should completely sequester Cu away from β2m and its oligomers. Upon removing Cu(II) in this way, the dimer and tetramer completely dissociate (cf. Figs. 5B and 6). These data indicate that the presence of Cu(II) is necessary for the dimer and the tetramer to form, but it does not definitively address whether Cu is bound to the dimer and tetramer or whether simply access to Cu by the monomer is necessary for these oligomers to form. In other words, it is conceivable that Cu(II) binding to the monomer allows β2m to reach a state that enables formation of dimers and tetramers, but once forming this state Cu(II) is released from the oligomers. In such a scenario, sequestration of Cu(II) would simply shift the

equilibrium back to the monomeric state, and the oligomers would eventually disappear. The MS data (Fig. 7B,C) rule out this scenario, though, and provide evidence that Cu(II) binding to the dimer and tetramer is necessary for their stability. The dimer and tetramer bind up to two and four Cu(II) ions, respectively. These Cu(II) ions are almost certainly bound specifically. Nonspecific binding is precluded because the samples were desalted prior to MS analysis, which would have removed uncomplexed Cu(II). Furthermore, analysis of lysozyme, which does not bind Cu(II), under identical conditions results in no measurable Cu adducts for this protein. The importance of Cu(II) for oligomer stability and the observation of Cu(II)-specific binding to these oligomers indicate that Cu(II) is required to maintain the intermolecular contacts between the dimers and the initial form of the tetramers.

A third important observation is that after about 5 d of incubation, some but not all of the tetramer remains after Cu(II) is sequestered by EDTA (Fig. 6). Very recently it was also reported that after a similar reaction time some β2m oligomers appear to lose their requirement for Cu(II) (Calabrese and Miranker 2007). Our results indicate that this occurs with the tetramer. Furthermore, our results indicate that there are two forms of the tetramer; one that binds Cu and one that does not. Unfortunately, the Cu(II)-binding status of the hexamer is unclear. As a likely product of this second tetramer form, insight into the Cu(II) content of the hexamer would be insightful. Higher-resolution MS measurements will be needed to determine directly whether or not Cu(II) binds to the hexamer.

A fourth important set of experimental observations is the temporal progression of the oligomers, which provides new information about the mechanism of β2m fibril formation. The DLS data (Fig. 3) are particularly illustrative in this regard; however, the MS data are roughly consistent with the DLS data. Close examination of the concentration changes of the oligomers over time provides two new insights. First, the concentration change of the tetramer over time is consistent with there being two forms of this oligomer. Second, the failure to consistently see soluble oligomers larger than the hexamer suggests that an oligomer just larger than the hexamer might be the unstable nucleus necessary for subsequent fibril formation. The key observations that support the idea of two tetrameric forms are the differences in how the concentrations of the dimer, tetramer, and hexamers change over time. The dimer forms before the tetramer (Figs. 3, 4C), and it appears that, when the dimer's concentration reaches a maximum, the rate of tetramer formation is the greatest (Fig. 3). These observations suggest that the dimer is a necessary precursor of the tetramer and that the tetramer begins to form as soon as dimer is present in solution. In contrast, the hexamer does not form until day 3 or 4, which is 2–3 d after the tetramer first appears. This observation may imply that the tetramer needs to go through some structural transition before the hexamer can form. This second form of the tetramer is also suggested by the EDTA addition experiments with SEC. By SEC, the second form of the tetramer, which does not bind Cu, is not observed until day 5; failure to observe it at day 3 or 4 is most likely due to the limited sensitivity that the SEC experiments have for the oligomers. An appealing way to reconcile the DLS, MS, and SEC observations is to speculate that the tetramer must reach a state in which Cu(II) is no longer bound before converting to the hexamer. The data further indicate that the tetramer's concentration continues to increase after the hexamer is formed, and this might be due to the buildup of the first tetramer that has not yet converted to the second tetrameric form that is required to progress to larger oligomeric species.

A second possible conclusion from the data in Figure 3 is that the nucleus necessary for subsequent fibril or protofibril formation could be an oligomer just larger than the hexamer. Nucleation-dependent aggregation is one of the hallmarks of amyloid fibrillogenesis (Rochet and Lansbury Jr. 2000), and oligomeric protein forms could be possible seeds. In the present case, the hexamer could be the largest stable oligomer possible before the formation of an unstable oligomeric nucleus ($[\beta 2m]_n$ where $n > 6$). An unstable oligomeric nucleus would not be experimentally observed presumably because of its very low steady-state concentration. Several observations support the idea of a nucleus that is just larger than the hexamer: (1) No octamers or decamers are observed, and only occasionally are dodecamers observed, which may form from the infrequent annealing of two hexamers; (2) the first indication of insoluble material occurs after 4 d of incubation, which coincides with the appearance of the hexamers in solution; (3) the first definitive evidence for amyloid-like fibrils occurs after 1 wk, which is when the hexamer concentration is at a maximum; (4) a significant drop in the concentrations of monomers and dimers in solution occurs upon the formation of the hexamers, presumably indicating a rapid conversion of soluble monomers and dimers into insoluble oligomer/aggregates after a species just larger than the hexamer is formed. While these experimental data suggest that the nucleus could be an oligomer just larger than the hexamer, more careful kinetic studies are needed to further confirm this hypothesis.

Proposed model for β2m fibril formation

The data presented here allow a more detailed model of Cu(II)-induced β2m fibril formation to be proposed (Fig. 8). In β2m, His31 (Eakin et al. 2002; Lim and Vachet

2004), the N-terminal amine (Lim and Vachet 2004), and possibly an amide nitrogen between Ile1 and Gln2 (Lim and Vachet 2004) comprise the Cu(II) binding site at pH = 7.4, although Cu(II) binding to His13 and His51 have also been suggested at lower pH values (Verdone et al. 2002; Villanueva et al. 2004). Both urea and thermal denaturation studies indicate that the conformational stability of β2m is lower in the presence of Cu(II) (Morgan et al. 2001; Eakin et al. 2002). Thus, Cu(II) destabilizes monomeric β2m (Fig. 8, **1**) and causes it to form a dimer (Fig. 8, **2**) and subsequently tetramer A (Fig. 8, **3**). The exact nature of the conformational change necessary for initial oligomer formation has not been determined for the wild-type protein, but it has recently been suggested that a *cis-trans* isomerization involving Pro32 caused by nearby Cu(II) is the necessary conformational change that allows oligomerization (Eakin et al. 2006). The same conformational change has been suggested to be a direct precursor for fibril elongation of β2m as well (Jahn et al. 2006). Furthermore, it has been suggested that β2m oligomers are formed via a domain-swapping mechanism (Eakin et al. 2004, 2006; Eakin and Miranker 2005). From the data presented here, the importance of Cu(II) to the stability of the dimer and tetramer A is evident from the experiments involving EDTA, which demonstrate these oligomers can revert back to monomers if Cu(II) is removed. A key step in the eventual formation of fibrils or protofibrils is the conversion of tetramer A into tetramer B (Fig. 8, **4**). The EDTA-addition experiments and the absence of Cu in the mature fibrils suggest that this conversion occurs via the loss of Cu(II). Evidently, stepwise association of β2m molecules provides the necessary energy to overcome the enthalpic penalty of Cu(II) dissociation. Conversion to tetramer B then allows the formation of the hexamer (Fig. 8, **5**). Our data do not indicate the oligomeric species that combines with tetramer B to form the hexamer, but the absence of any pentamers or octamers might suggest the involvement of a dimer. Once the hexamer is formed, we hypothesize that a slightly larger oligomer acts as the nucleus (Fig. 8, **6**) that enables fibril or protofibril formation (Fig. 8, **7**).

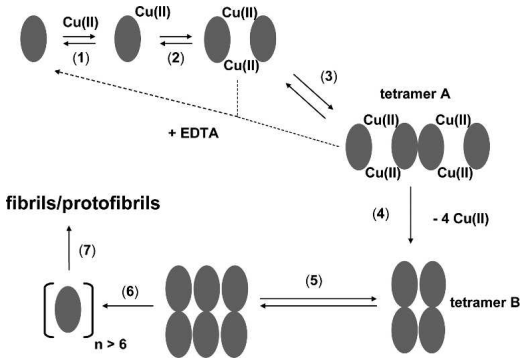

Figure 8. Proposed model for the role of Cu(II) and β2m oligomers in amyloid fibril formation.

If correct, then there are three important implications of this model. First, β2m amyloid formation is preceded by discrete oligomeric intermediates. Further structural characterization of these intermediates, especially the two tetrameric forms and the hexamer, may identify rational strategies to prevent β2m fibril formation. Second, this model suggests that formation of the nucleus is not completely responsible for the lag phase observed with fibril formation of β2m. A structural transition [i.e., Cu(II) loss] by a prior intermediate accounts for some of the lag phase. Third, Cu(II) is only necessary for nucleation and is released from β2m upon fibril formation. This observation indicates that biologically relevant concentrations of Cu may be sufficient for β2m fibril formation in vivo. Significant concentrations of Cu(II) in joint spaces of dialysis patients may not be necessary to cause β2m fibril formation at these sites. Instead, interactions between β2m and Cu(II) at other locations (e.g., dialysate) may be sufficient to form the nucleus that is the necessary precursors to fibrils.

Materials and Methods

Materials

Wild-type β2m was obtained from Fitzgerald Industries International, Inc. The protein was purified by ultrafiltration with Centricon 10,000 molecular-weight cutoff centrifuge tubes (Millipore Corp.) prior to use. Urea and nitric acid were obtained from Mallinckrodt Baker, Inc. 3-(*N*-morpholino)propanesulfonic acid (MOPS) and all other proteins were obtained from Sigma-Aldrich. All other chemicals were obtained from Fisher Scientific. Deionized water from a Millipore Simplicity 185 water purification system was used for all sample preparations.

Formation of β2m fibrils

To obtain the amyloid fibrils of β2m, a sample solution containing 100 μM β2m, 200 μM copper(II) sulfate, 200 mM potassium acetate, 500 mM urea, and 25 mM MOPS (pH 7.4) was incubated at 37°C. Control experiments without Cu(II) were also performed in which a solution containing 100 μM β2m, 10 mM ethylenediamine tetraacetic acid (EDTA), 200 mM potassium acetate, 500 mM urea, and 25 mM MOPS (pH 7.4) was also incubated at 37°C. EDTA was added to ensure no association between trace amounts of Cu(II) and the protein.

Size-exclusion chromatography

The compounds present in incubated solutions of β2m were separated using a Superdex 75 PC 3.2/30 column (Amersham Biosciences) installed on an HP 1100 series high-performance liquid chromatography system (Agilent). Before analysis of the

sample, the SEC column was first equilibrated with a 20 mM ammonium acetate mobile phase (pH = 7.4) at a 0.04 mL/min flow rate for 1 h. During the analysis, 5 μL of an incubated sample solution was injected into the sample loop. A variable-wavelength detector set at 280 nm was used for detection. For the molecular weight (MW) calibration, a solution containing a mixture of the following proteins and peptides was used: 1.5 μM bovine serum albumin (MW = 66,000), 3 μM carbonic anhydrase (MW = 29,040), 3 μM β2m (MW = 11,731), and 30 μM angiotensin I (MW = 1296). For online SEC-ESI-MS experiments, 20 μL of sample was injected onto the column. The high-energy MS source conditions, which are described below, were used for these online analyses.

Desalting

Desalting experiments were performed using a 5-mL HiTrap desalting column from Amersham Biosciences that had an exclusion limit of 5000 Da. The column was first equilibrated with 30 mL of the mobile phase (10 mM ammonium acetate, pH 7.4). Then, 100 μL of the incubated sample was injected onto the column via a sample loop attached to a homemade setup. The desalted β2m sample was eluted at a flow rate of 5 mL/min using 10 mM ammonium acetate (pH 7.4), which was filled into a syringe and delivered by a peristaltic pump. About 20 s after injection of the sample, ~1.0 mL of the β2m fraction eluting from the column was collected and then analyzed within ~2 min by ESI-MS. Not only did the desalting column remove excess salt that would compromise subsequent ESI-MS analyses, but it also reduced the total concentration of the protein to less than 10 μM, which was important for minimizing nonspecific complex formation during the ESI process.

Mass spectrometry

A JMS-700 MStation (JEOL) double-focusing mass spectrometer equipped with a standard ESI source was used to acquire all mass spectra. Two different ESI source conditions were used. For the low-energy source conditions, the following settings were used: desolvating plate temperature, 100°C; orifice temperature, 140°C; orifice potential, 0 V; ring lens potential, 100 V. For the high-energy source conditions, the following settings were used: desolvating plate temperature, 100°C; orifice temperature, 140°C; orifice potential, 60 V; ring lens potential, 100 V.

Dynamic light scattering (DLS)

DLS studies were conducted using a Zetasizer Nano-ZS instrument (Malvern Instruments). The intensity of the scattered laser was measured by optics placed at 173°. Measurements were performed using 45 μL of incubated sample. Before analysis of each sample, the device was pre-equilibrated at 37°C for 5 min and was maintained at this temperature throughout the experiment. Every sample was measured five times for 0.5 min each, and at least three replicate measurements were performed for each incubation time point. The CONTIN algorithm was used to fit the resulting intensity correlation curves as multi-exponentials. Essential to the success of these measurements was careful transfer of the incubated sample into the DLS instrument. Excessive agitation of the sample prior to analysis resulted in the data being completely dominated by particles with diameters >100 nm. To minimize the suspension of insoluble material in the solutions interrogated by DLS, the sample was centrifuged at 14,000*g* for 8 min prior to analysis.

Thioflavin T fluorescence

Fluorescence experiments were performed using a QuantaMaster 4 SE spectrofluorometer (Photon Technology International). A solution containing 100 μM β2m, 80 μM ThT, 500 mM urea, 25 mM MOPS, and 200 mM potassium acetate was initially equilibrated at 37°C, and after addition of 200 μM $CuSO_4$, the fluorescent enhancement of ThT was measured. Measurements were taken at excitation and emission wavelengths of 437 and 483 nm, respectively.

Transmission electron microscopy (TEM)

TEM images were obtained on a JEOL JEM-100CX electron microscope operating at 100 keV. Before analysis, a solution containing insoluble material was centrifuged (14,000*g*) for 8 min and decanted, and the solid material was resuspended in 10 μL of the supernatant. The resulting solution was then applied to carbon-coated copper grids and allowed to air-dry for 5 min. The sample was then stained with 1% phosphotungstic acid, air-dried for 12 h, and then viewed.

Inductively coupled plasma mass spectrometry

Copper was determined with an ELAN DRC-e (PerkinElmer Instruments) ICP mass spectrometer, equipped with a cross-flow nebulizer, a Scott-type double-pass spray chamber, and a quadrupole mass filter. The instrument was used in peak hopping mode, with ~0.05 s residence time per mass, and a total analysis time of 1.24 min per run. Flow injection was used to introduce an incubated β2m sample for analysis. The sample injection volume was 150 μL. Working standard solutions of copper, obtained by serial dilution from a stock solution, were prepared in 1% sub-boiled nitric acid. A 1000 mg/L stock solution of Cu(II) was prepared by dissolving 0.1965 g of $CuSO_4 \cdot 5H_2O$ in 50 mL 1% nitric acid. The reported measurements were obtained using a gallium internal standard. The internal standard was prepared from a stock solution of 1 mg/L gallium in 1% nitric acid, which was obtained from 0.5 mL of a 1000 mg/L atomic absorption standard solution (Ricca Chemical Co.).

X-ray microanalysis

A JEOL 6320 FXV field emission scanning electron microscope (FESEM) was used for the X-ray microanalysis experiments on β2m fibrils. This FESEM instrument is equipped with a BE (backscattered) detector and a thin-window energy-dispersive X-ray spectrometer from Princeton Gamma-Tech, which enables X-ray microanalysis on sub-micrometer-sized samples. The voltage used in the analysis of the β2m fibrils was 10 kV, the tilt angle was 20°, and the beam current was 8 μA. β2m fibrils were washed several times with buffer before X-ray analysis.

Acknowledgments

This work was supported by a grant from the National Institutes of Health (RO1 GM075092). We thank Louis Raboin for his

help with the X-ray microanalysis experiments, Professor Paul Dubin and Basak Kayitmazer for access to and help with the dynamic light scattering instrument, and Professor David Reckhow for access to the ICP-MS instrument.

References

Bjorkman, P.J., Saper, M.A., Samraoui, B., Bennett, W.S., Strominger, J.L., and Wiley, D.C. 1987. Structure of the human class-I histocompatibility antigen, HLA-A2. *Nature* **329:** 506–512.

Bush, A.I. and Tanzi, R.E. 2002. The galvanization of β-amyloid in Alzheimer's disease. *Proc. Natl. Acad. Sci.* **99:** 7317–7319.

Calabrese, M.F. and Miranker, A.D. 2007. Formation of a stable oligomer of β-2 microglobulin requires only transient encounter with Cu(II). *J. Mol. Biol.* **367:** 1–7.

Connors, L.H., Shirahama, T., Skinner, M., Fenves, A., and Cohen, A.S. 1985. *In vitro* formation of amyloid fibrils from intact β-2-microglobulin. *Biochem. Biophys. Res. Commun.* **131:** 1063–1068.

Davis, D.P., Gallo, G., Vogen, S.M., Dul, J.L., Sciarretta, K.L., Kumar, A., Raffen, R., Stevens, F.J., and Argon, Y. 2001. Both the environment and somatic mutations govern the aggregation pathway of pathogenic immunoglobulin light chain. *J. Mol. Biol.* **313:** 1021–1034.

Drüeke, T.B. 2000. β_2-Microglobulin and amyloidosis. *Nephrol. Dial. Transplant.* **15:** 17–24.

Eakin, C.M. and Miranker, A.D. 2005. From chance to frequent encounters: Origins of β2-microglobulin fibrillogenesis. *Biochim. Biophys. Acta* **1753:** 92–99.

Eakin, C.M., Knight, J.D., Morgan, C.J., Gelfand, M.A., and Miranker, A.D. 2002. Formation of a copper specific binding site in nonnative states of β-2-microglobulin. *Biochemistry* **41:** 10646–10656.

Eakin, C.M., Attenello, F.J., Morgan, C.J., and Miranker, A.D. 2004. Oligomeric assembly of native-like precursors precedes amyloid formation by β-2 microglobulin. *Biochemistry* **43:** 7808–7815.

Eakin, C.M., Berman, A.J., and Miranker, A.D. 2006. A native to amyloidogenic transition regulated by a backbone trigger. *Nat. Struct. Mol. Biol.* **13:** 202–208.

Esposito, G., Michelutti, R., Verdone, G., Viglino, P., Hernandez, H., Robinson, C.V., Amoresano, A., Dal Piaz, F., Monti, M., Pucci, P., et al. 2000. Removal of the N-terminal hexapeptide from human β2-microglobulin facilitates protein aggregation and fibril formation. *Protein Sci.* **9:** 831–845.

Ferrao-Gonzales, A.D., Robbs, B.K., Moreau, V.H., Ferreira, A., Juliano, L., Valente, A.P., Almeida, F.C.L., Silva, J.L., and Foguel, D. 2005. Controlling β-amyloid oligomerization by the use of naphthalene sulfonates—trapping low molecular weight oligomeric species. *J. Biol. Chem.* **280:** 34747–34754.

Floege, J. and Ketteler, M. 2001. β_2-Microglobulin-derived amyloidosis: An update. *Kidney Int.* **59:** S164–S171. doi: 10.1093/ndt/gfm712.

Friedhoff, P., von Bergen, M., Mandelkow, E.-M., Davies, P., and Mandelkow, E. 1998. A nucleated assembly mechanism of Alzheimer paired helical filaments. *Proc. Natl. Acad. Sci.* **95:** 15712–15717.

Goldstein, J.I., Newbury, D.E., Echlin, P., Joy, D.C., Romig, A.D., Lyman, C.E., Fiori, C., and Lifshin, E. 1992. *Scanning electron microscopy and x-ray microanalysis: A text for biologists, materials scientists, and geologists*, 2d ed. Plenum Press, New York.

Jahn, T.R., Parker, M.J., Homans, S.W., and Radford, S.E. 2006. Amyloid formation under physiological conditions proceeds via a native-like folding intermediate. *Nat. Struct. Mol. Biol.* **13:** 195–201.

Jobling, M.F., Huang, X., Stewart, L.R., Barnham, K.J., Curtain, C., Volitakis, I., Perugini, M., White, A.R., Cherny, R.A., Masters, C.L., et al. 2001. Copper and zinc binding modulates the aggregation and neurotoxic properties of the prion peptide PrP106–126. *Biochemistry* **40:** 8073–8084.

Kirkitadze, M.D., Bitan, G., and Teplow, D.B. 2002. Paradigm shift in Alzheimer's disease and other neurodegenerative disorders: The emerging role of oligomeric assemblies. *J. Neurosci. Res.* **69:** 567–577.

Lim, J. and Vachet, R.W. 2004. Using mass spectrometry to study copper-protein binding under native and nonnative conditions: β-2-microglobulin. *Anal. Chem.* **76:** 3498–3504.

McParland, V.J., Kad, N.M., Kalverda, A.P., Brown, A., Kirwin-Jones, P., Hunter, M.G., Sunde, M., and Radford, S.E. 2000. Partially unfolded states of β_2-microglobulin and amyloid formation in vitro. *Biochemistry* **39:** 8735–8746.

Morgan, C.J., Gelfand, M., Atreya, C., and Miranker, A.D. 2001. Kidney dialysis-associated amyloidosis: A molecular role for Cu(II) in fiber formation. *J. Mol. Biol.* **309:** 339–345.

Naiki, H., Higuchi, K., Hosokawa, M., and Takeda, T. 1989. Fluorometric determination of amyloid fibrils in vitro using the fluorescent dye, thioflavin T. *Anal. Biochem.* **177:** 244–249.

Ohhashi, Y., Kihara, M., Naiki, H., and Goto, Y. 2005. Ultrasonication-induced amyloid fibril formation of β_2-microglobulin. *J. Biol. Chem.* **280:** 32843–32848.

Relini, A., Canale, C., De Stefano, S., Rolandi, R., Giorgetti, S., Stoppini, M., Rossi, A., Fogolari, F., Corazza, A., Esposito, G., et al. 2006. Collagen plays an active role in the aggregation of β_2-microglobulin under physiopathological conditions of dialysis-related amyloidosis. *J. Biol. Chem.* **281:** 16521–16529.

Rochet, J.C. and Lansbury Jr., P.T. 2000. Amyloid fibrillogenesis: Themes and variations. *Curr. Opin. Struct. Biol.* **10:** 60–68.

Smith, A.M., Jahn, T.R., Ashcroft, A.E., and Radford, S.E. 2006. Direct observation of oligomeric species formed in the early stages of amyloid fibril formation using electrospray ionisation mass spectrometry. *J. Mol. Biol.* **364:** 9–19.

Uversky, V.N., Li, J., and Fink, A.L. 2001. Metal-triggered structural transformations, aggregation, and fibrillation of human α-synuclein. A possible molecular link between Parkinson's disease and heavy metal exposure. *J. Biol. Chem.* **276:** 44284–44296.

Verdone, G., Corazza, A., Viglino, P., Pettirossi, F., Giorgetti, S., Mangione, P., Andreola, A., Stoppini, M., Bellotti, V., and Esposito, G. 2002. The solution structure of human β2-microglobulin reveals the prodromes of its amyloid transition. *Protein Sci.* **11:** 487–499.

Villanueva, J., Hoshino, M., Katou, H., Kardos, J., Hasegawa, K., Naiki, H., and Goto, Y. 2004. Increase in the conformational flexibility of β_2-microglobulin upon copper binding: A possible role for copper in dialysis-related amyloidosis. *Protein Sci.* **13:** 797–809.

Wadsworth, J.D., Hill, A.F., Joiner, S., Jackson, G.S., Clarke, A.R., and Collinge, J. 1999. Strain-specific prion-protein conformation determined by metal ions. *Nat. Cell Biol.* **1:** 55–59.

Walsh, D.M., Lomakin, A., Benedek, G.B., Condron, M.M., and Teplow, D.B. 1997. Amyloid β-protein fibrillogenesis—detection of a protofibrillar intermediate. *J. Biol. Chem.* **272:** 22364–22372.